Highlights of Spanish Astrophysics XII, Proceedings of the XVI Scientific Meeting of the Spanish Astronomical Society held on July 15 - 19, 2024, in Granada, Spain. M. Manteiga, F. González Galindo, A. Labiano Ortega, M. Martínez González, N. Rea, M. Romero Gómez, A. Ulla Miguel, G. Yepes, C. Rodríguez López, A. Gómez García and C. Dafonte (eds.), 2025

Debris disks around mature M dwarf stars

Baraibar, O.[1], Anglada, G.[1], Osorio, M.[1], Gómez, J. F.[1], Blázquez-Calero, G.[1], Amado, P. J.[1]

[1] Instituto de Astrofísica de Andalucía, CSIC, Glorieta de la Astronomía s/n, E-18008 Granada, Spain

Abstract

Debris disks are reservoirs of gas and dust made up of the leftover material from planetary formation. Most research on debris disks has focused on young stars, but Gyr-old stars are also expected to host these disks. Here, we present Atacama Compact Array (ACA) 1.3 mm observations toward three M-dwarf stars with known exoplanet candidates: GJ 191, GJ 273, and GJ 581. The goal of this study is to detect the presence of residual material which can help to investigate how dynamical evolution of the planetary systems may have contributed to the dispersal of dust grains within these disks.

1 Introduction

In the past three decades, approximately 6000 exoplanets have been confirmed (NASA Exoplanet Archive), deepening our understanding of exoplanetary systems. A key aspect of exoplanetary systems, often forgotten, is the presence of gas and dust, either left over from planet formation or generated by collisions between large bodies ("collisional cascade", [20]). Minor bodies such as comets, asteroids and dust grains from micron to km sizes, form the debris disk of a star.

Planetary systems can undergo chaotic dynamical evolution due to gravitational interactions among their planets, leading to the scattering of dust grains [20]. Such chaotic dynamic interactions are thought to have occurred in the Solar System, where the original Kuiper belt (with a mass of 35 $M_\oplus$ [7]) and Asteroid Belt, became ∼3% and ∼10% of their original masses, respectively (Nice Model, [13, 7, 17]). A similar process could have occurred to other exoplanetary systems, producing a more depleted debris disk with respect to the original one.

2 Target stars

In order to have a more complete understanding of exoplanetary systems, it is helpful to search for debris disks around stars with known planetary systems. Given the low mass and abundance of M dwarf stars, the detection of exoplanets by radial velocity and transit methods around them is favored. Therefore, among these stars, we have selected three nearby candidates to search for dust emission at millimeter wavelengths, in order to maximize the sensitivity of our observations.

The selected targets are three nearby planet-hosting Gyr-old M dwarf stars: GJ 191, GJ 273 and GJ 581. The coordinates of the sources along with their proper motions, their distances and stellar characteristics such as the spectral type, luminosity, effective temperature, mass, radius and age are listed in Table 1.

Table 1: Properties of the target stars

	GJ 191	GJ 273	GJ 581
α (ICRS[a])	$05^h\ 11^m\ 50.38496^s$	$07^h\ 27^m\ 25.11083^s$	$15^h\ 19^m\ 25.51232^s$
δ (ICRS[a])	$-45°\ 02'\ 37.7257''$	$05°\ 12'\ 33.7777''$	$-07°\ 43'\ 21.7453''$
μ_α cosδ (mas/yr)	6491.22	571.23	−1221.28
μ_δ (mas/yr)	−5708.61	−3691.49	−97.23
Distance (pc)	3.934	3.786	6.300
Spectral type	M1.0V	M3.5V	M3.0V
L_* ($L_\odot$)	0.0124	0.0088	0.0123
$T_{\rm eff}$ (K)	3570	3382	3500
M_* ($M_\odot$)	0.281	0.29	0.295
R_* ($R_\odot$)	0.291	0.293	0.302
Age (Gyr)	>10	>8	2-8
References	[5, 6, 16]	[5, 8, 2, 4, 14]	[5, 15, 3, 12, 18, 10]

[a] Reference Epoch J2016.0.

3 Observations

The observations of GJ 191, GJ 273 and GJ 581 were carried out with Atacama Compact Array (ACA) at 1.3 mm (Band 6) under the project 2017.1.01644.S (PI: P. J. Amado). We used four spectral windows centered at 224, 226, 240, and 242 GHz, each one with a 2 GHz bandwidth split into 120 channels. The observations were conducted between January 5 and September 29 of 2018 for GJ 191; from November 29 of 2017 to April 8 of 2018 for GJ 273; and from August 31 to September 21 of 2018 for GJ 581. At the wavelength of observations, the primary beam (FWHM) is $\sim 39''$.

Since the observations of each target spanned weeks to months, the phase center was updated in each scan to track the variation on the coordinates of the source due to large proper motions and parallax. They were also considered for the combination of the data of each system. The coordinates assigned to the source are the ones of the first observing epoch.

Version 5.4.0-68 of the Common Astronomy Software Applications (CASA) package was used for data processing. Calibration of ACA data was performed by ALMA pipeline. The images of the three sources were obtained by combining the four spectral windows using the CONCAT task of CASA, applying a "natural" weighting, and deconvolving with the CLEAN algorithm. The synthesized beam and sensitivity achieved are: beam = $7.28'' \times 4.44''$ (PA = 88.0°) and rms=30 μJy/beam for GJ 191; beam = $7.22'' \times 4.51''$ (PA = -88.3°) and rms=26 μJy/beam for GJ 273; beam = $7.24'' \times 4.44''$ (PA = -82.5°) and rms=34 μJy/beam for GJ 581. Further details of the observations can be found in [1].

4 Results

We have detected 1.3 mm emission towards all three sources. The observed flux density is the sum of the flux density of the star and that of the disk of dust. The stellar flux at 1.3 mm was calculated under the assumption that the star radiates as a black body at its effective temperature, and, if an excess emission is detected, we attribute it to thermal emission from the dust surrounding the star. In Figures 1, 2,3 we plot the expected Spectral Energy Distribution (SED) and the flux densities measured at different wavelengths.

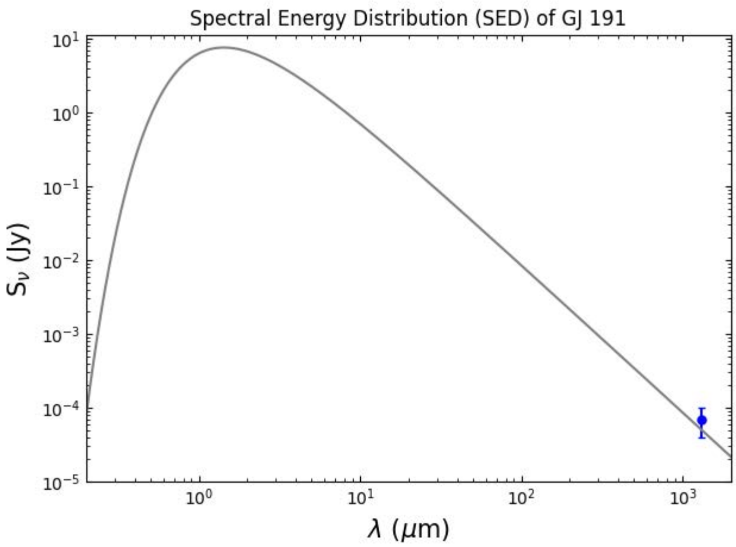

Figure 1: SED of the star GJ 191, modeled as a black body at the effective temperature $T_{\rm eff}$=3570 K, stellar radius R_*=0.291 $R_\odot$ and a distance of 3.934 pc (see Table 1). The flux density measured at 1.3 mm from our ACA observations, S_ν=70±30 μJy, is marked in blue. Adapted from [1].

GJ 191: The measured flux density is 70±30 μJy and it has a flux excess of ∼19±30 μJy with respect to the expected SED of the star at the observation wavelength of 1.3 mm (Figure 1), suggesting that there is no significant dust emission associated with this source.

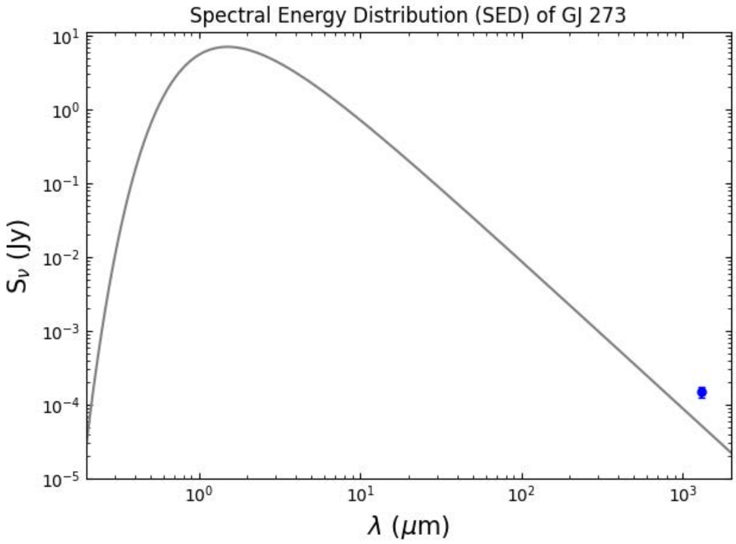

Figure 2: SED of the star GJ 273, modeled as a black body at the effective temperature $T_{\rm eff}$=3382 K, stellar radius R_*=0.293 $R_\odot$ and a distance of 3.786 pc (see Table 1). The flux density measured at 1.3 mm by our ACA observations, S_ν=150±26 μJy, is marked in blue. Adapted from [1].

Table 2: Photometry of GJ 581

λ (μm)	S_ν (mJy)	Instrument	Reference
9.0	322±18	AKARI	[9]
11.6	213±19	WISE	[19]
22.1	61.2±6	WISE	[19]
70.0	18.9±1.4	PACS, HSO[a]	[10]
100.0	21.5±1.5	PACS, HSO[a]	[10]
160.0	22.2±5.0	PACS, HSO[a]	[10]
250.0	<24	SPIRE, HSO[a]	[10]
350.0	<26	SPIRE, HSO[a]	[10]
500.0	<27	SPIRE, HSO[a]	[10]
1200.0	<2.1	MAMBO, IRAM	[11]
1300.0	0.68±0.09	ACA	[1]

[a] Herschel Space Observatory

GJ 273: The measured flux density is 150±26 μJy with a flux excess of ∼97±26 μJy with respect to the expected SED of the star at 1.3 mm (Figure 2), suggesting that a faint debris disk is associated with this source. This faint disk, could be the result of the chaotic dynamical evolution of the exoplanetary system.

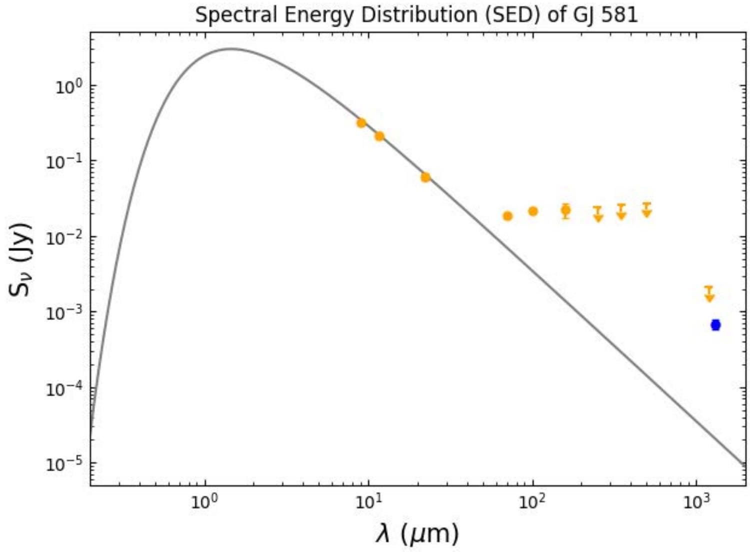

Figure 3: SED of the star GJ 581, modeled as a black body at the effective temperature $T_{\rm eff}$=3500 K, stellar radius R_*=0.302 $R_\odot$ and a distance of 6.300 pc (see Table 1). The flux density measurements at infrared wavelengths and at 1.2 mm (Table 2) are plotted in orange. The flux density measured at 1.3 mm by our ACA observations, S_ν=680±90 μJy, is marked in blue. Adapted from [1].

GJ 581: In Table 2 we show all the available measurements of the flux density of GJ 581 system obtained from the literature, as well as our ACA measurement at 1.3 mm. Figure 3 shows the SED of the star, modeled as a black body, as well as the flux measurements shown in Table 2, where a strong infrared and millimeter excess can be seen. The measured flux density is 680±90 μJy with a flux excess of ∼660±90 μJy with respect to the expected SED of the star at 1.3 mm. This suggests that the debris disk has not suffered a strong depletion as a result of dynamical interactions among the planets of the system.

The detection of dust in certain mature systems, while absent in others, indicates that planetary systems may experience different dynamical evolution. Further discussion can be found in [1].

Acknowledgments

This paper makes use of the following ALMA data: ADS/JAO.ALMA#2017.1.01644.S ALMA is a partnership of ESO (representing its member states), NSF (USA) and NINS (Japan), together with NRC (Canada), MOST and ASIAA (Taiwan), and KASI (Republic of Korea), in cooperation with the Republic of Chile. The Joint ALMA Observatory is operated by ESO, AUI/NRAO and NAOJ. The National Radio Astronomy Observatory is a facility of the National Science Foundation operated under cooperative agreement by Associated Universities, Inc. This work is supported by grants PID2020-114461GB-I00, PID2023-146295NB-I00, and CEX2021-001131-S, funded by MCIN/AEI /10.13039/501100011033. Part of this work was presented at the symposium "On the origin of stars and their planets: A holistic view" within the framework of the SEA2024.

References

[1] Baraibar, O., Anglada, G., Osorio, M., et al., in preparation

[2] Boyajian, T. S., von Braun, K., van Belle, G., et al. 2012, AJ, 757, 112

[3] Cifuentes, C. 2023, PhD thesis, Complutense University of Madrid, Spain

[4] Delfosse, X., Forveille, T., Ségransan, D., et al. 2000, A&A, 364, 217

[5] Gaia Collaboration, Brown, A. G. A., Vallenari, A., et al. 2021, A&A, 649, A1

[6] Gizis, J. E. 1997, AJ, 113, 806

[7] Gomes, R., Levison, H. F., Tsiganis, K., & Morbidelli, A. 2005, Nature, 435, 466

[8] Hawley, S. L., Gizis, J. E., & Reid, I. N. 1996, AJ, 112, 2799

[9] Ishihara, D., Onaka, T., Kataza, H., et al. 2010, A&A, 514, A1

[10] Lestrade, J.-F., Matthews, B., Sibthorpe, B., et al. 2012, A&A, 548, A86

[11] Lestrade, J.-F., Wyatt, M. C., Bertoldi, F., Menten, K. M., & Labaigt, G. 2009, A&A, 506, 1455

[12] Marfil, E., Tabernero, H. M., Montes, D., et al. 2021, A&A, 656, A162

[13] Morbidelli, A., Levison, H., Tsiganis, K., & Gomes, R. 2005, Nature, 435, 462

[14] Pozuelos, F. J., Suárez, J. C., de Elía, G. C., et al. 2020, A&A, 641, A23

[15] Reid, I. N., Hawley, S. L., & Gizis, J. E. 1995, AJ, 110, 1838

[16] Ségransan, D., Kervella, P., Forveille, T., & Queloz, D. 2003, A&A, 397, L5

[17] Tsiganis, K., Gomes, R., Morbidelli, A., & Levison, H. F. 2005, Nature, 435, 459

[18] von Stauffenberg, A., Trifonov, T., Quirrenbach, A., et al. 2024, A&A, 688, A112

[19] Wright, E. L., Eisenhardt, P. R. M., Mainzer, A. K., et al. 2010, AJ, 140, 1868

[20] Wyatt, M. C. 2008, ARA&A, 46, 339